Electronic Supplementary Information (ESI) for Dalton Transactions
This journal is © The Royal Society of Chemistry 2017

Supporting Information For

Rapid and highly sensitive detection of extracellular and intracellular H_2S by an azide-functionalized Al(III)-based metal-organic framework

*Soutick Nandi, Helge Reinsch, Sooram Banesh, Norbert Stock, Vishal Trivedi, and Shyam Biswas**

* To whom correspondence should be addressed.
E-mail: sbiswas@iitg.ernet.in. Tel: (+)91-3612583309. Fax: (+)91-3612582349.

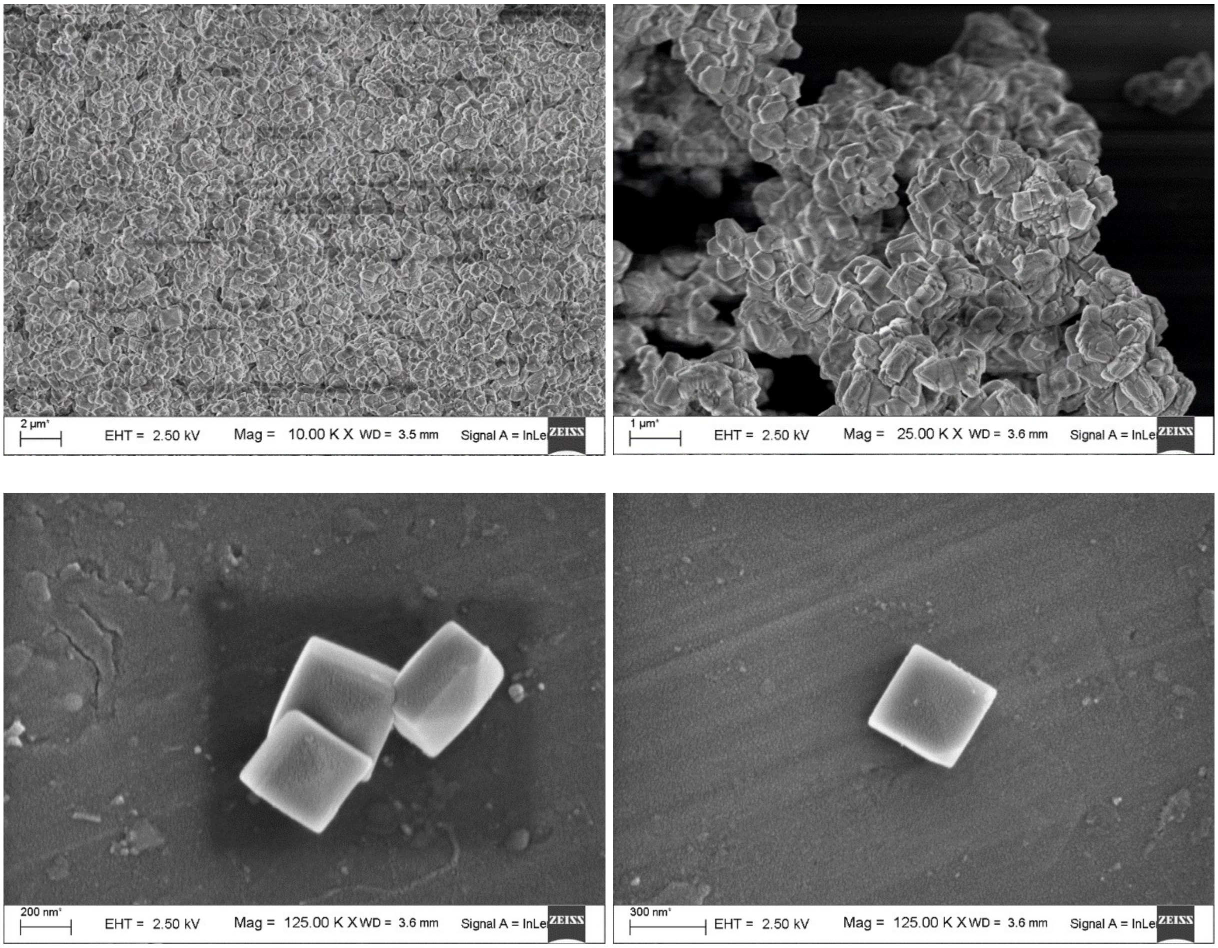

Figure S1. FE-SEM images of **1**.

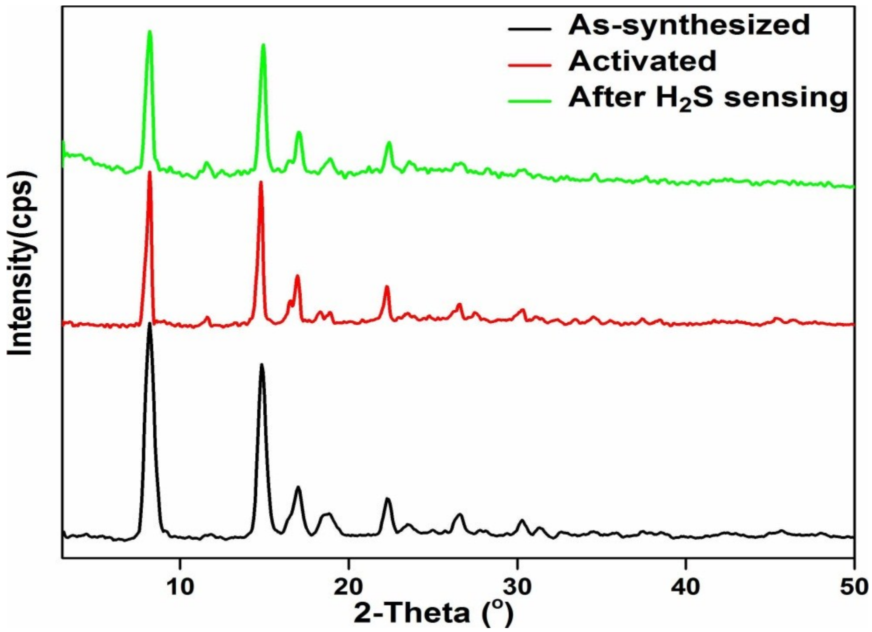

Figure S2. XRPD patterns of **1** in different forms: as-synthesized, thermally activated and after H_2S sensing experiment.

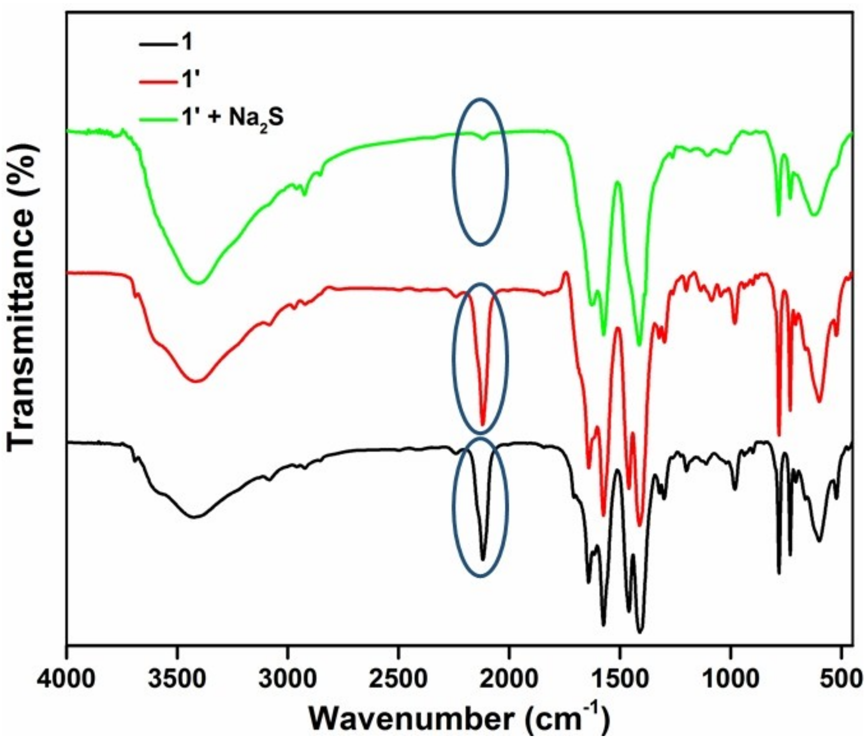

Figure S3. FT-IR spectra of as-synthesized **1** (black), activated (red) **1'**, and **1'** after treatment with Na_2S (green). The absorption bands for the $–N_3$ group are high-lighted by the blue ovals.

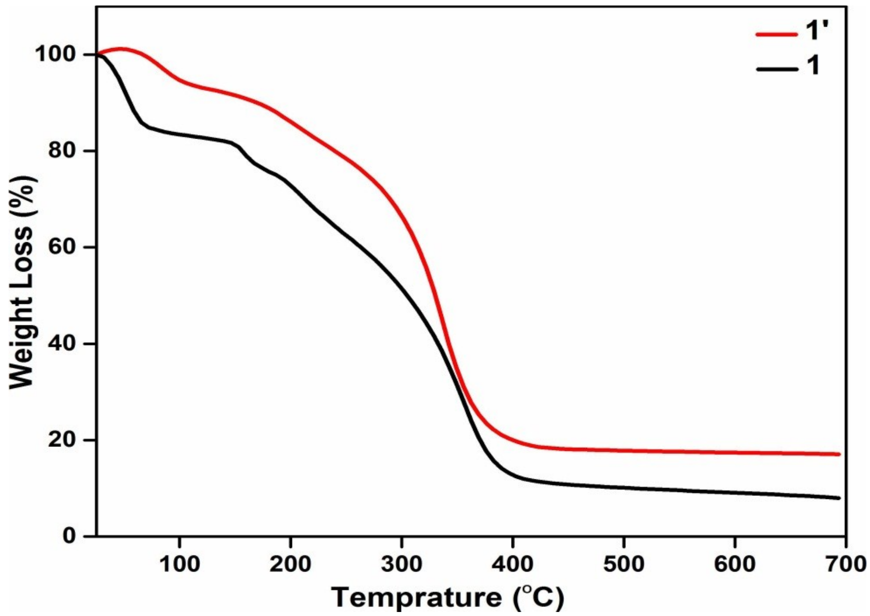

Figure S4. TG curves of as-synthesized **1** (black) and activated **1'** (red) recorded in an air atmosphere in the temperature range of 25-700 °C with a heating rate of 5 °C min^{-1}.

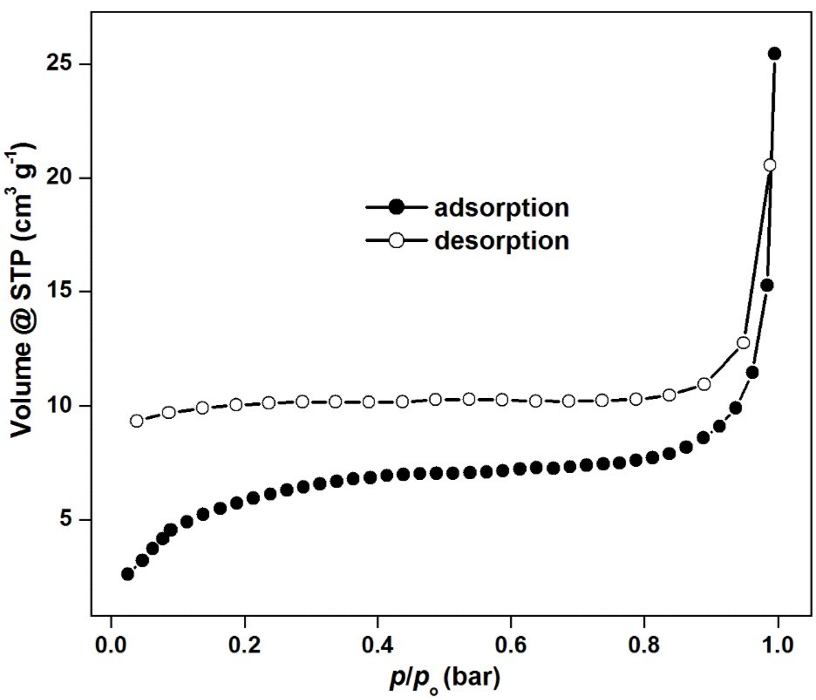

Figure S5. N_2 adsorption (solid symbols) and desorption (empty symbols) isotherms of thermally activated **1'** recorded at –196 °C.

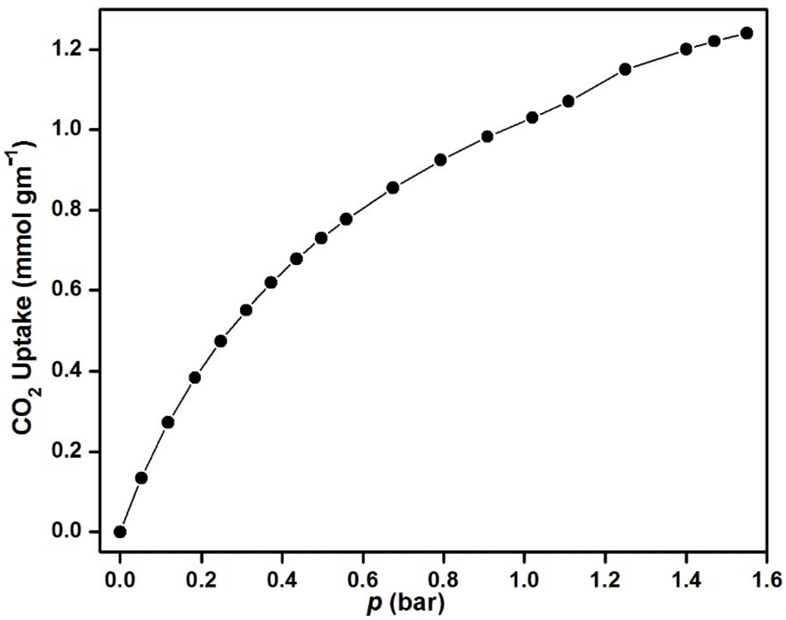

Figure S6. CO_2 adsorption isotherm of thermally activated **1'** recorded at 25 °C.

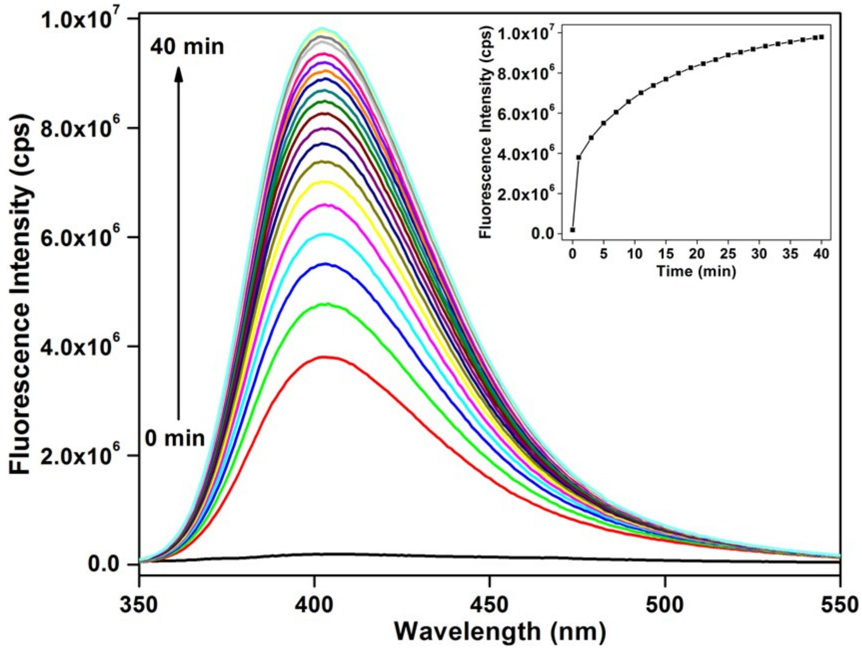

Figure S7. Fluorescence turn-on response of **1′** (in pure aqueous medium) towards gradual addition of Na_2S at a regular time interval of 1 min up to 40 min. Inset: time-dependence of the fluorescence emission intensity (λ_{ex} = 330 nm and λ_{em} = 405 nm).

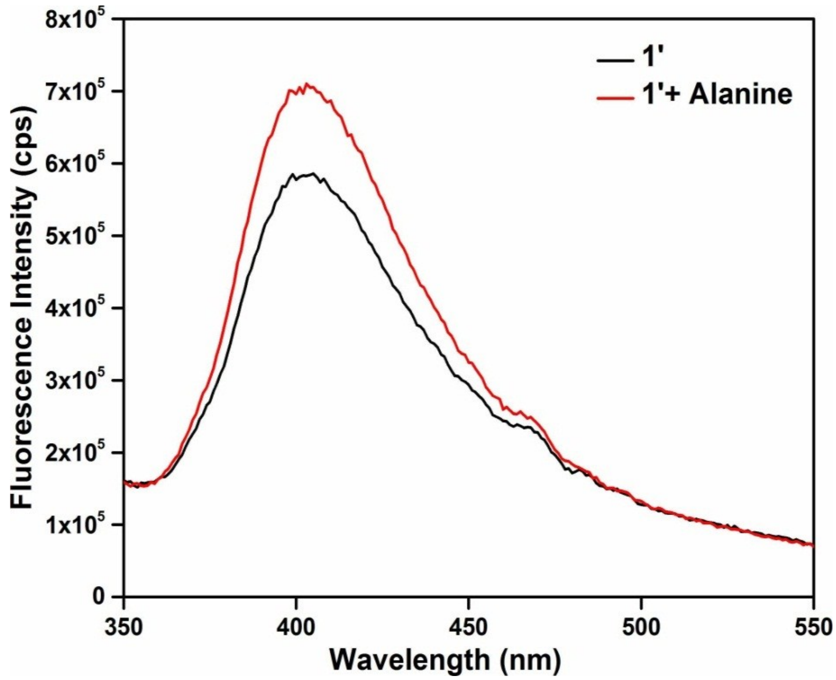

Figure S8. Fluorescence response of **1'** before (black) and after (red) addition of alanine at 15 min (λ_{ex} = 330 nm and λ_{em} = 405 nm).

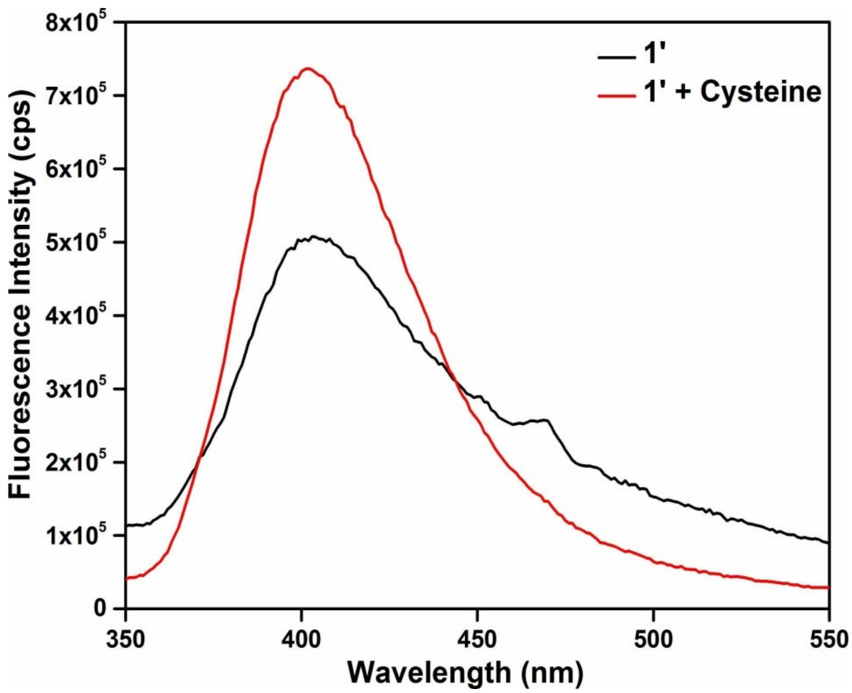

Figure S9. Fluorescence response of **1'** before (black) and after (red) addition of cysteine at 15 min (λ_{ex} = 330 nm and λ_{em} = 405 nm).

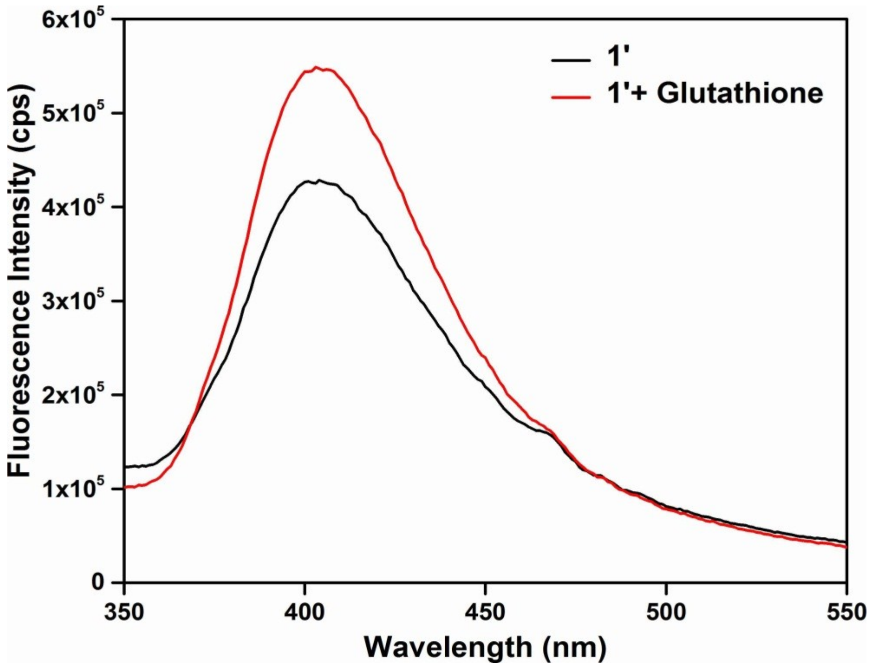

Figure S10. Fluorescence response of **1'** before (black) and after (red) addition of glutathione at 15 min (λ_{ex} = 330 nm and λ_{em} = 405 nm).

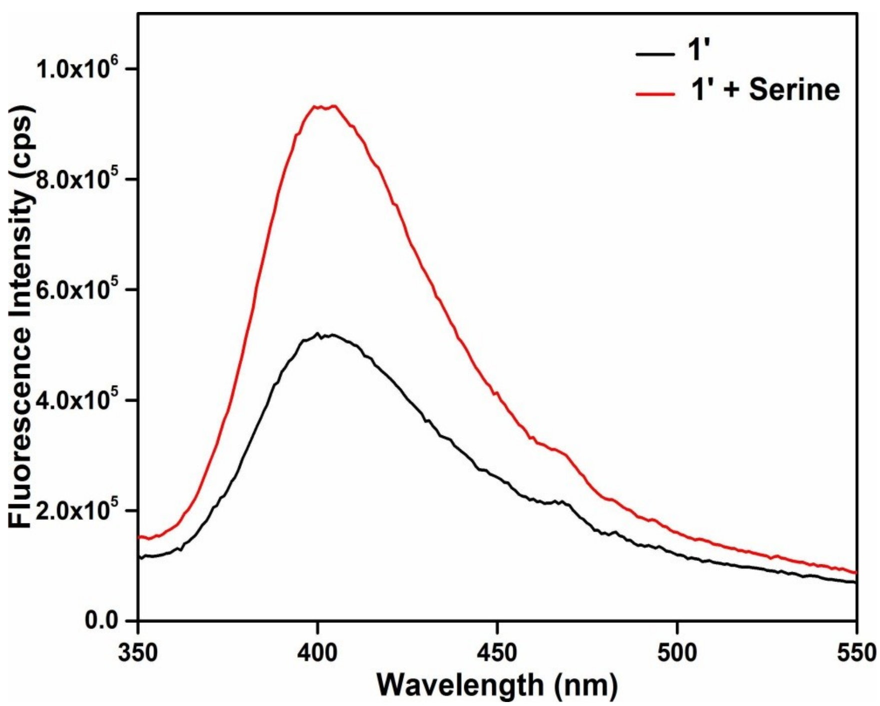

Figure S11. Fluorescence response of **1'** before (black) and after (red) addition of serine at 15 min (λ_{ex} = 330 nm and λ_{em} = 405 nm).

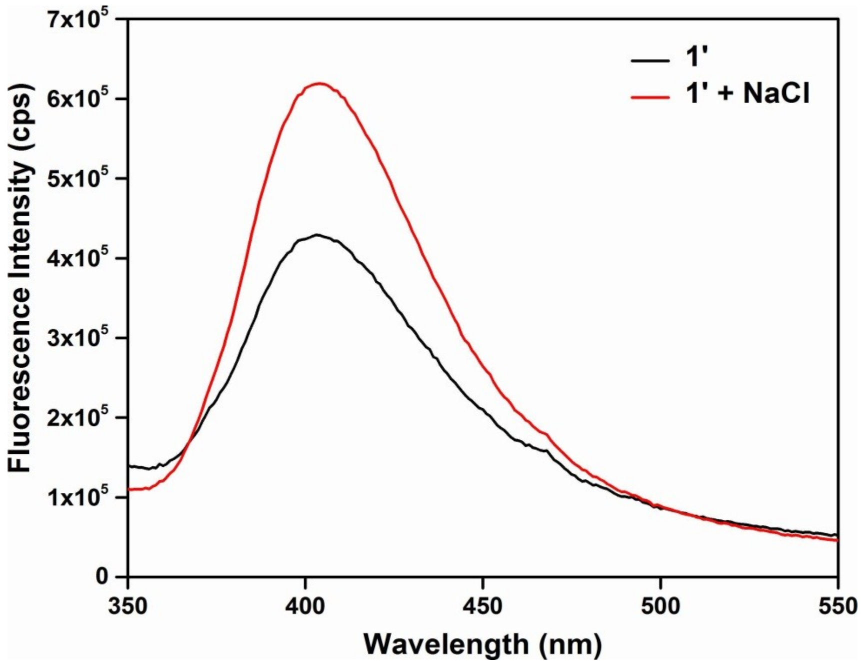

Figure S12. Fluorescence response of **1'** before (black) and after (red) addition of NaCl at 15 min (λ_{ex} = 330 nm and λ_{em} = 405 nm).

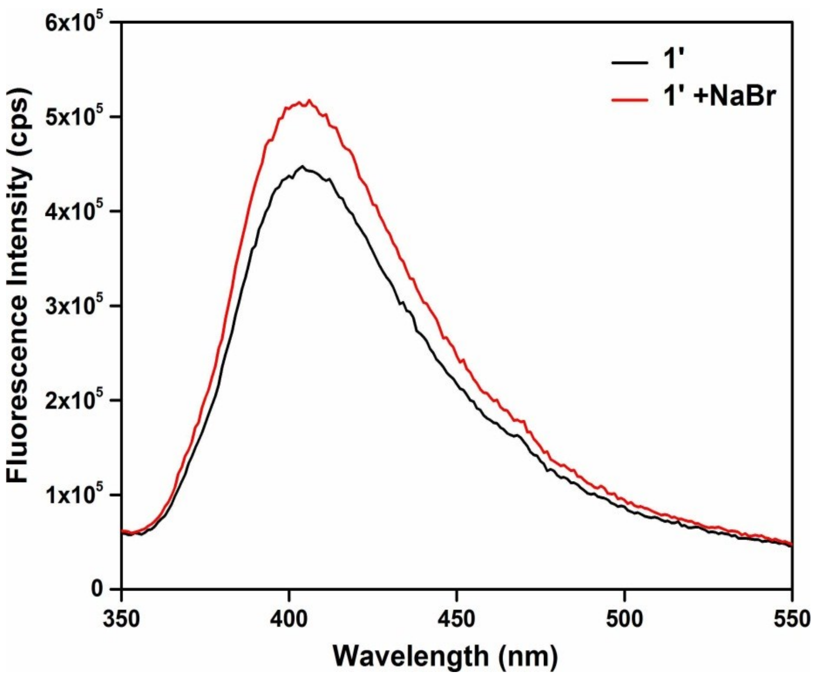

Figure S13. Fluorescence response of **1'** before (black) and after (red) addition of NaBr at 15 min (λ_{ex} = 330 nm and λ_{em} = 405 nm).

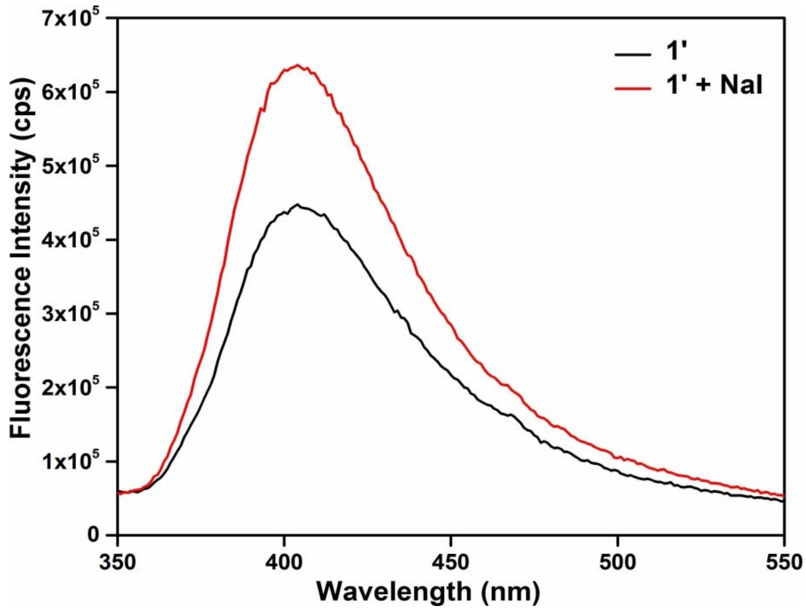

Figure S14. Fluorescence response of **1'** before (black) and after (red) addition of NaI at 15 min (λ_{ex} = 330 nm and λ_{em} = 405 nm).

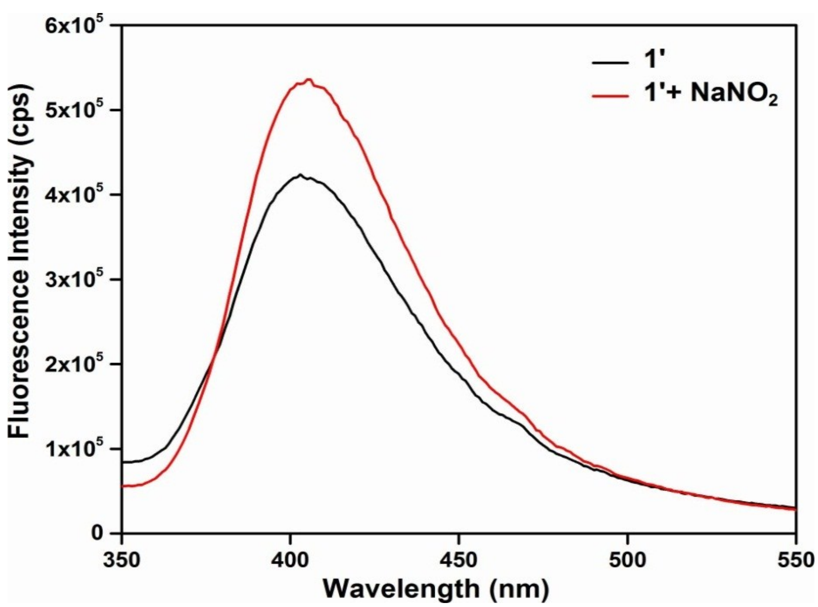

Figure S15. Fluorescence response of **1'** before (black) and after (red) addition of $NaNO_2$ at 15 min (λ_{ex} = 330 nm and λ_{em} = 405 nm).

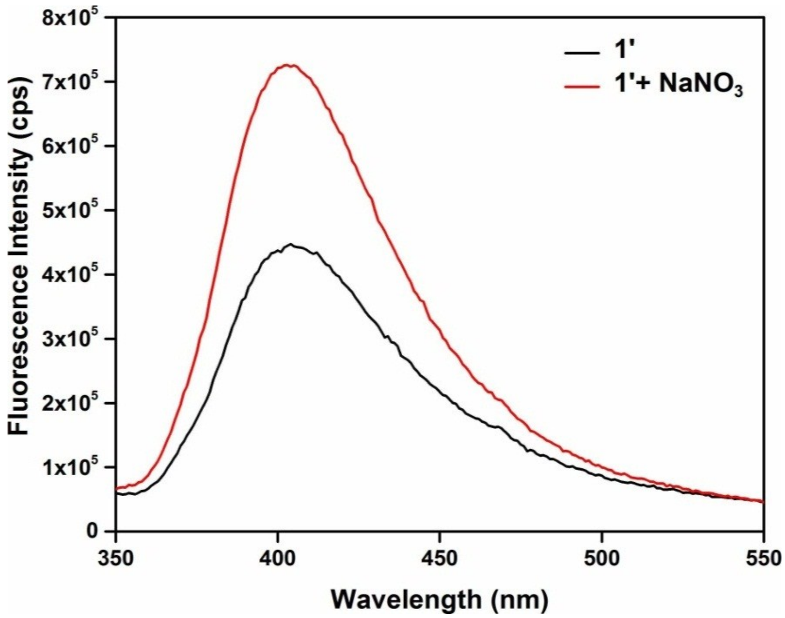

Figure S16. Fluorescence response of **1'** before (black) and after (red) addition of $NaNO_3$ at 15 min (λ_{ex} = 330 nm and λ_{em} = 405 nm).

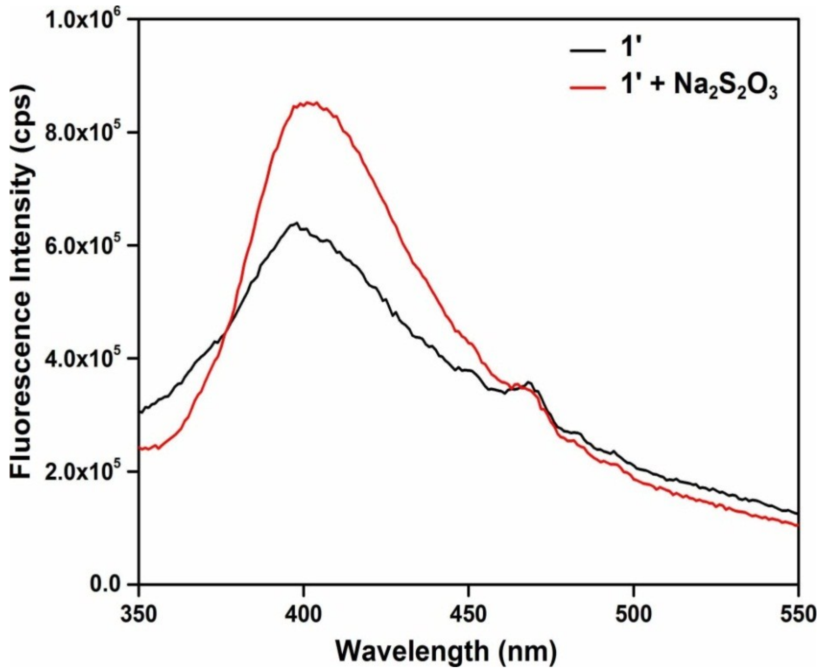

Figure S17. Fluorescence response of **1'** before (black) and after (red) addition of $Na_2S_2O_3$ at 15 min (λ_{ex} = 330 nm and λ_{em} = 405 nm).

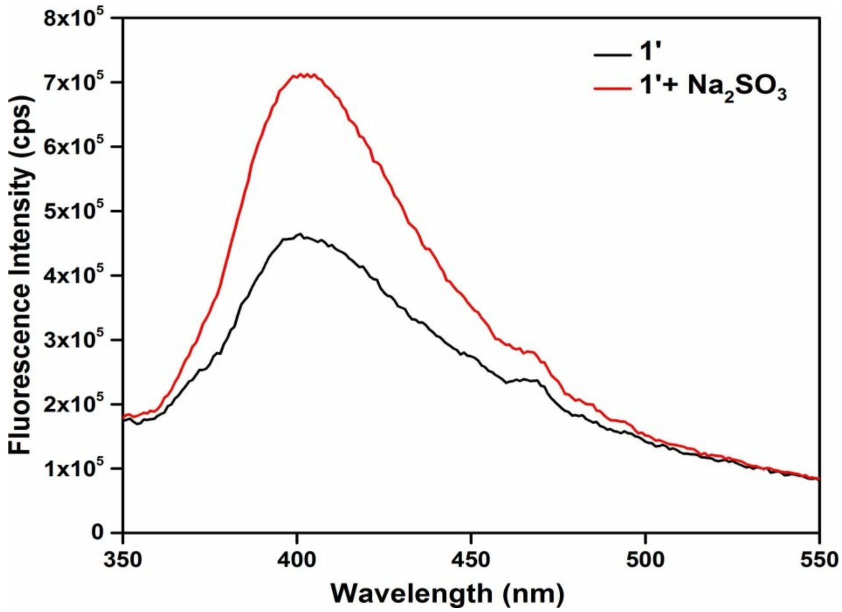

Figure S18. Fluorescence response of **1'** before (black) and after (red) addition of Na_2SO_3 at 15 min (λ_{ex} = 330 nm and λ_{em} = 405 nm).

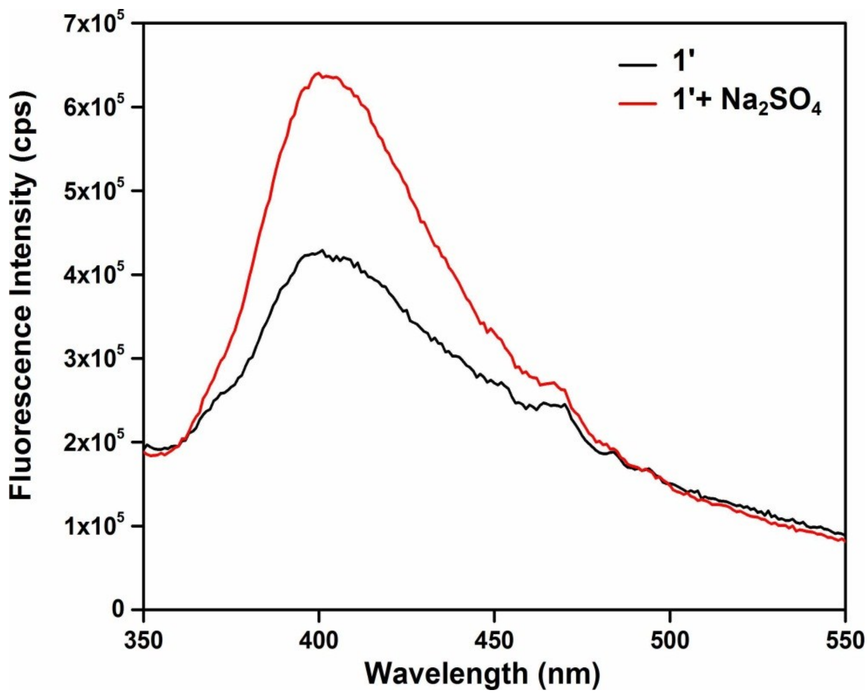

Figure S19. Fluorescence response of **1'** before (black) and after (red) addition of Na_2SO_4 at 15 min (λ_{ex} = 330 nm and λ_{em} = 405 nm).

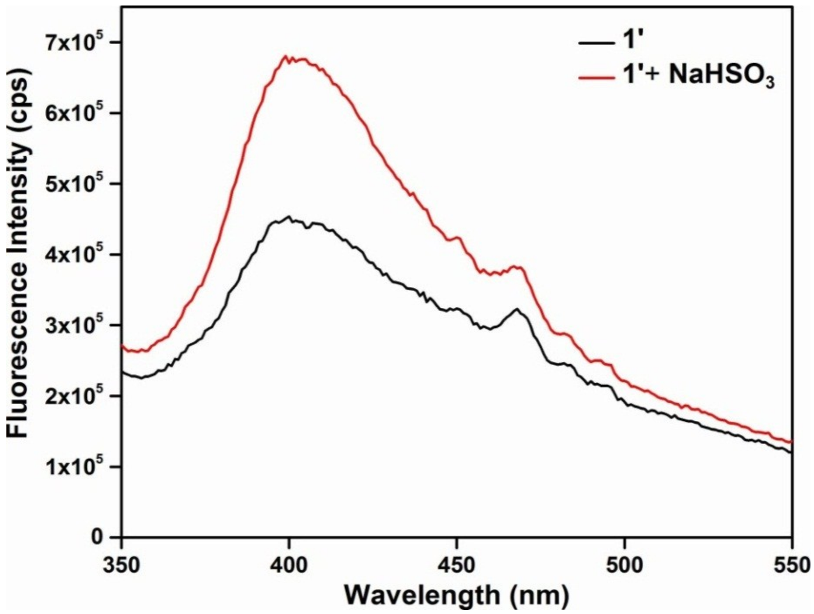

Figure S20. Fluorescence response of **1'** before (black) and after (red) addition of $NaHSO_3$ at 15 min (λ_{ex} = 330 nm and λ_{em} = 405 nm).

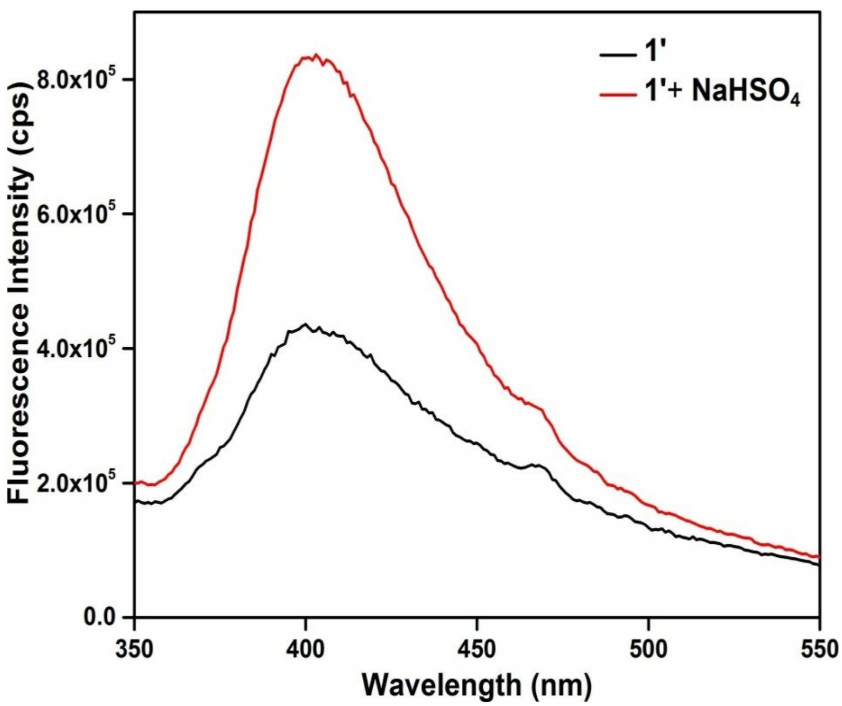

Figure S21. Fluorescence response of **1'** before (black) and after (red) addition of $NaHSO_4$ at 15 min (λ_{ex} = 330 nm and λ_{em} = 405 nm).

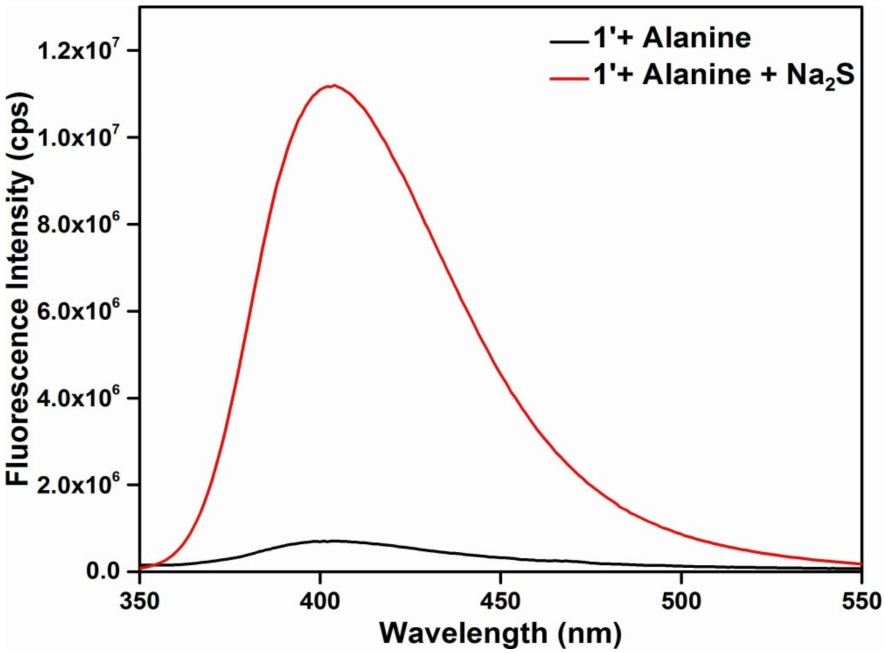

Figure S22. Fluorescence response of **1′** towards Na_2S in presence of alanine (λ_{ex} = 330 nm and λ_{em} = 405 nm).

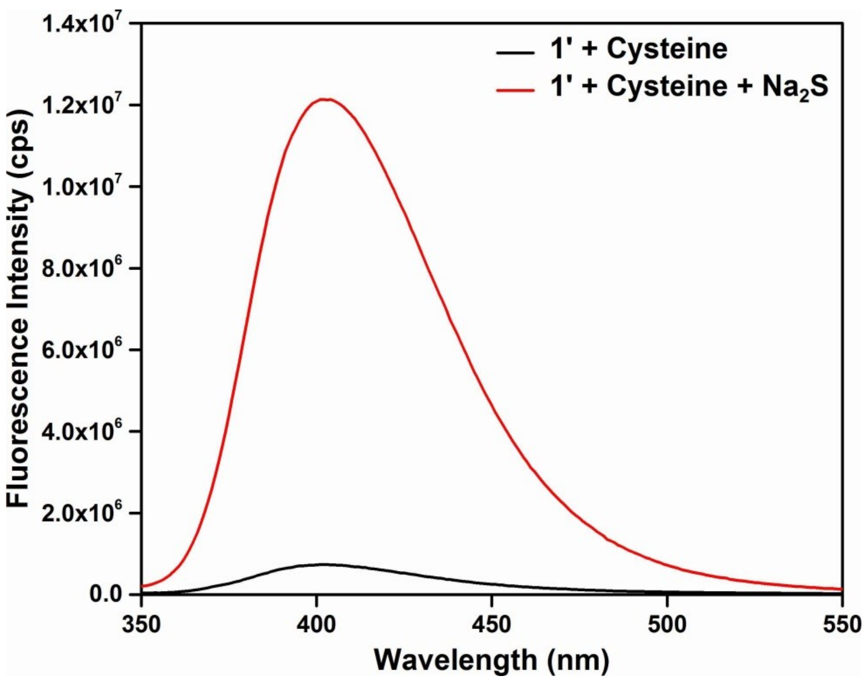

Figure S23. Fluorescence response of **1′** towards Na_2S in presence of cysteine (λ_{ex} = 330 nm and λ_{em} = 405 nm).

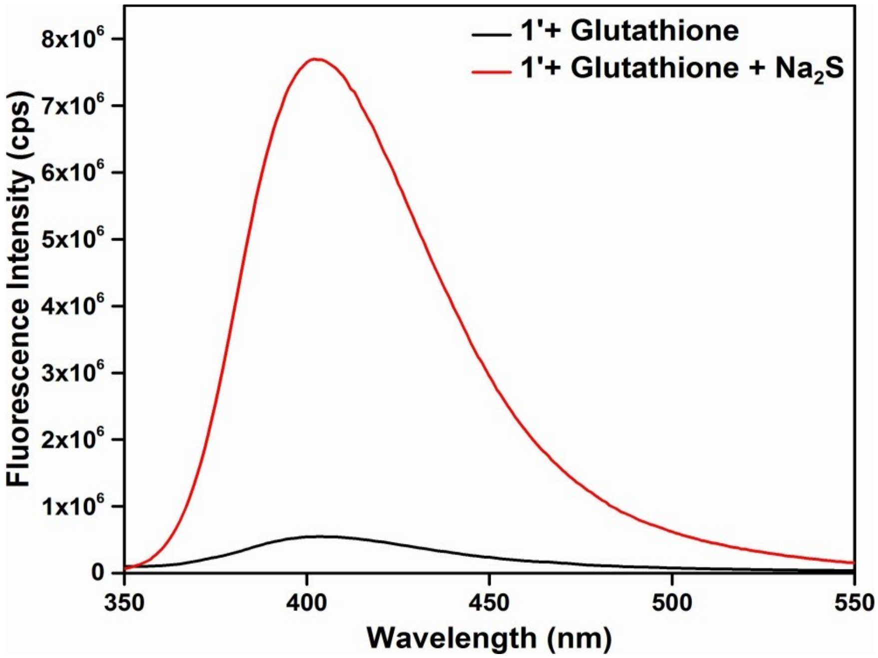

Figure S24. Fluorescence response of **1′** towards Na_2S in presence of glutathione (λ_{ex} = 330 nm and λ_{em} = 405 nm).

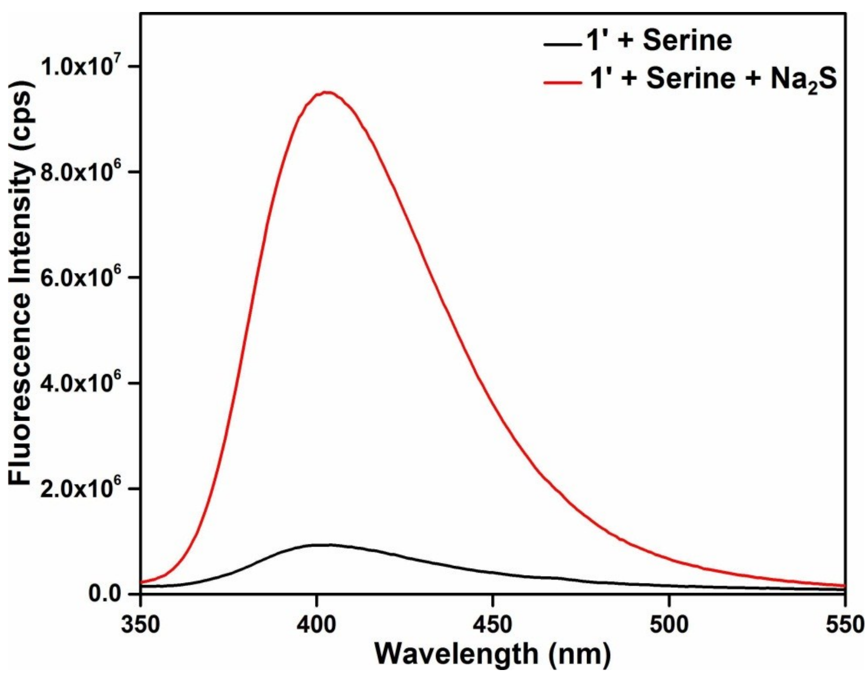

Figure S25. Fluorescence response of **1′** towards Na_2S in presence of serine (λ_{ex} = 330 nm and λ_{em} = 405 nm).

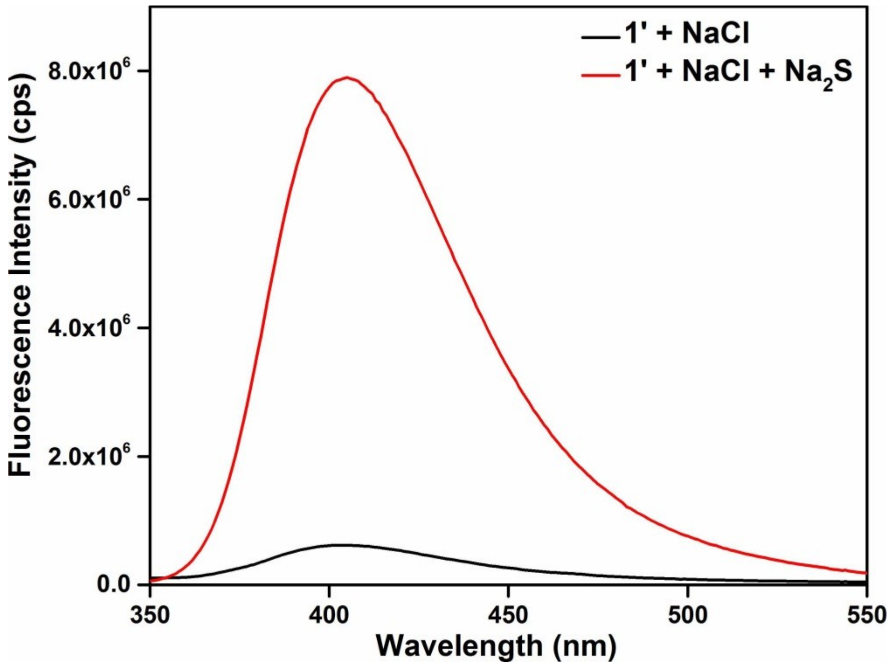

Figure S26. Fluorescence response of **1′** towards Na_2S in presence of NaCl (λ_{ex} = 330 nm and λ_{em} = 405 nm).

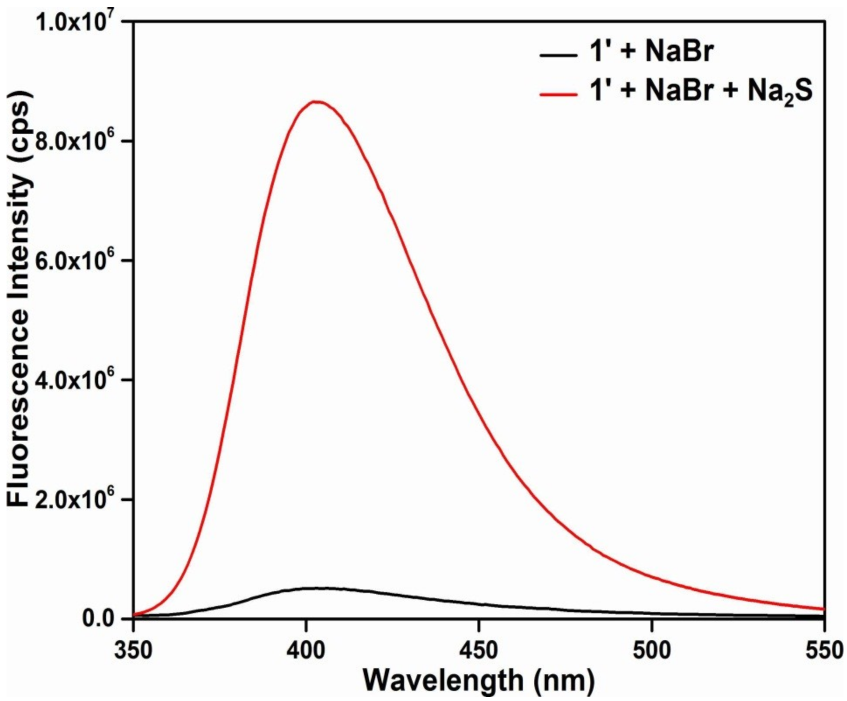

Figure S27. Fluorescence response of **1′** towards Na_2S in presence of NaBr (λ_{ex} = 330 nm and λ_{em} = 405 nm).

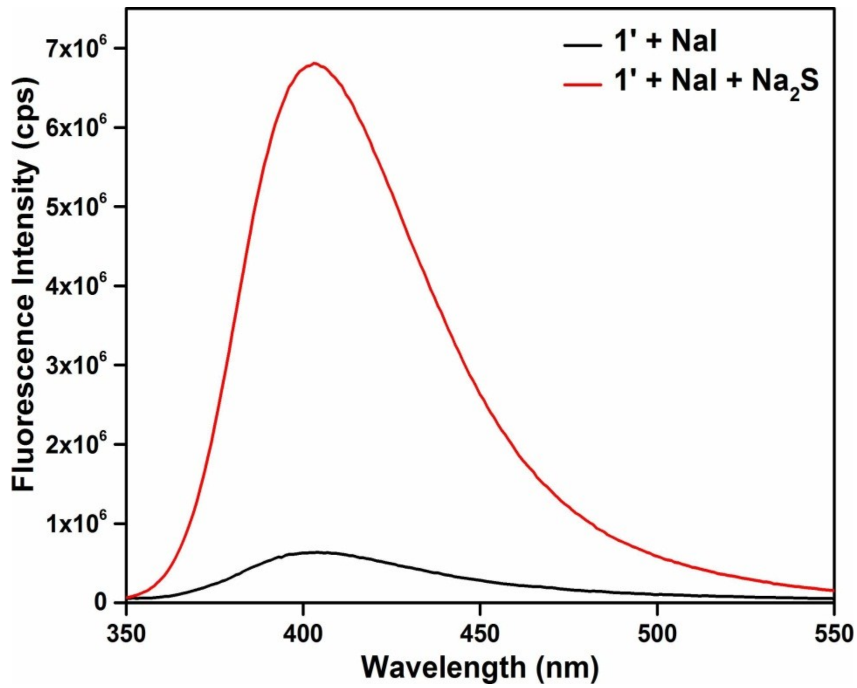

Figure S28. Fluorescence response of **1′** towards Na_2S in presence of NaI (λ_{ex} = 330 nm and λ_{em} = 405 nm).

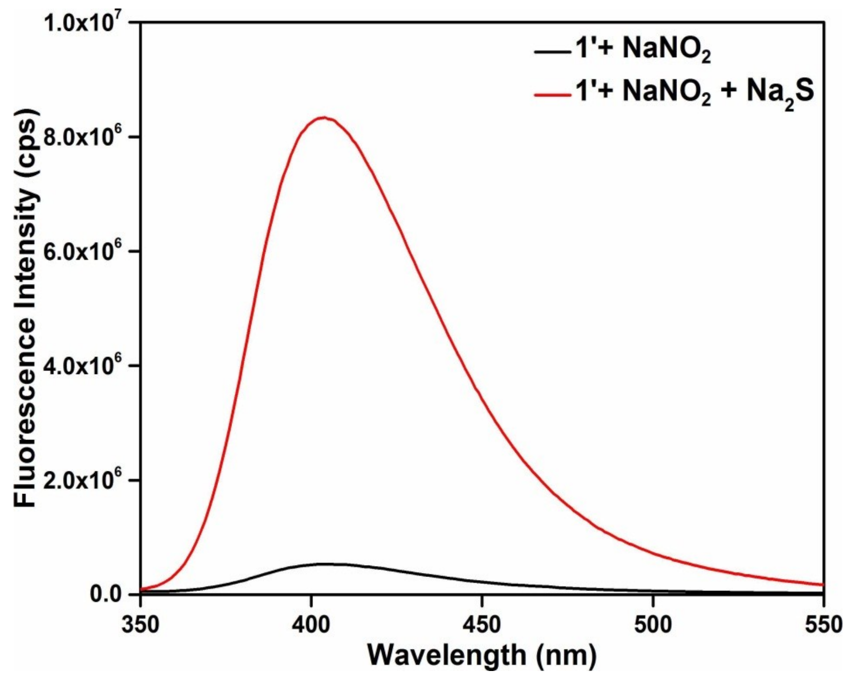

Figure S29. Fluorescence response of **1′** towards Na_2S in presence of $NaNO_2$ (λ_{ex} = 330 nm and λ_{em} = 405 nm).

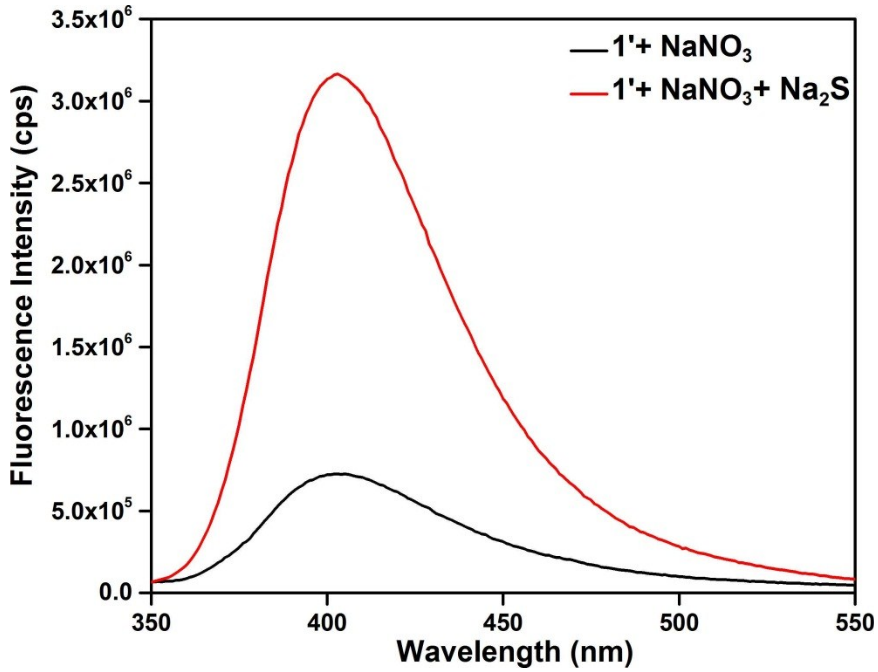

Figure S30. Fluorescence response of **1′** towards Na_2S in presence of $NaNO_3$ (λ_{ex} = 330 nm and λ_{em} = 405 nm).

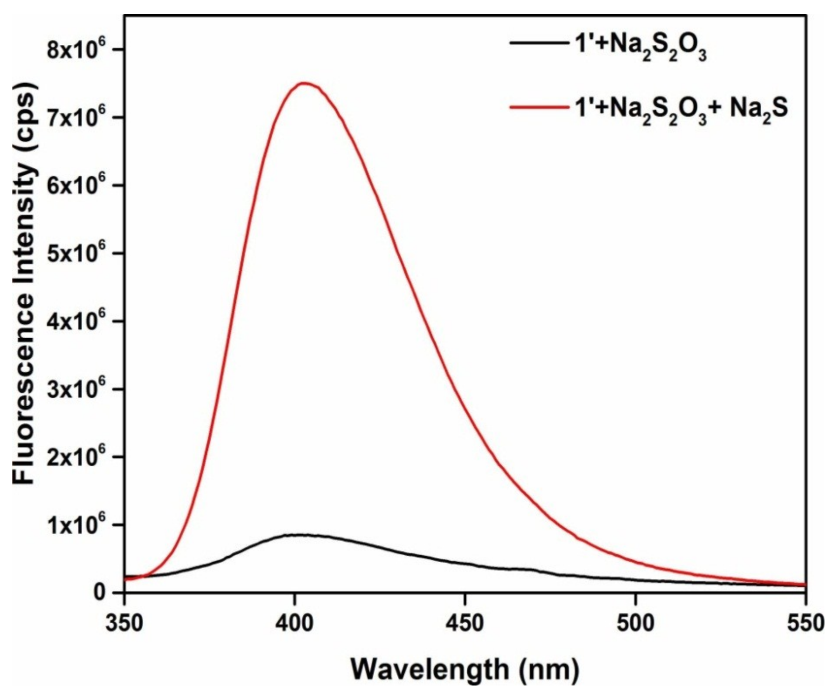

Figure S31. Fluorescence response of **1′** towards Na_2S in presence of $Na_2S_2O_3$ (λ_{ex} = 330 nm and λ_{em} = 405 nm).

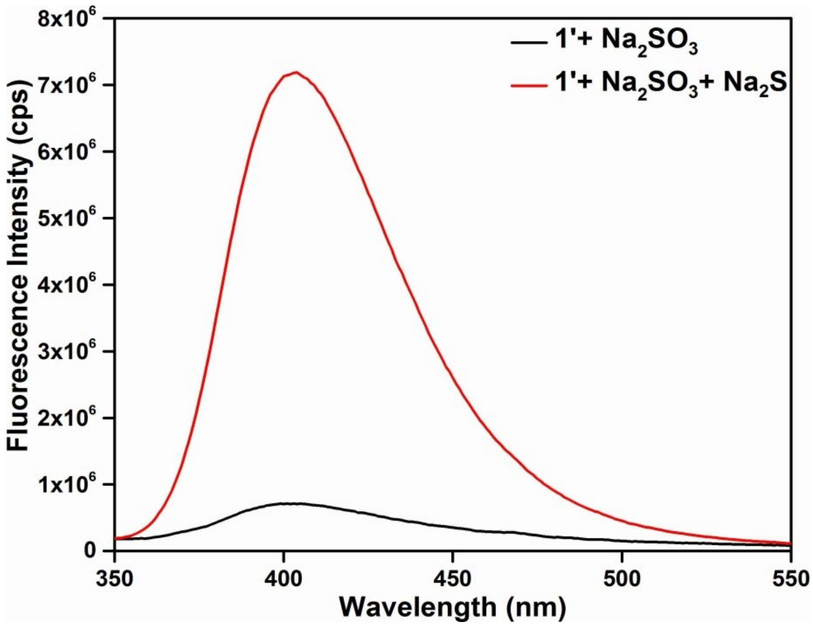

Figure S32. Fluorescence response of **1′** towards Na_2S in presence of Na_2SO_3 (λ_{ex} = 330 nm and λ_{em} = 405 nm).

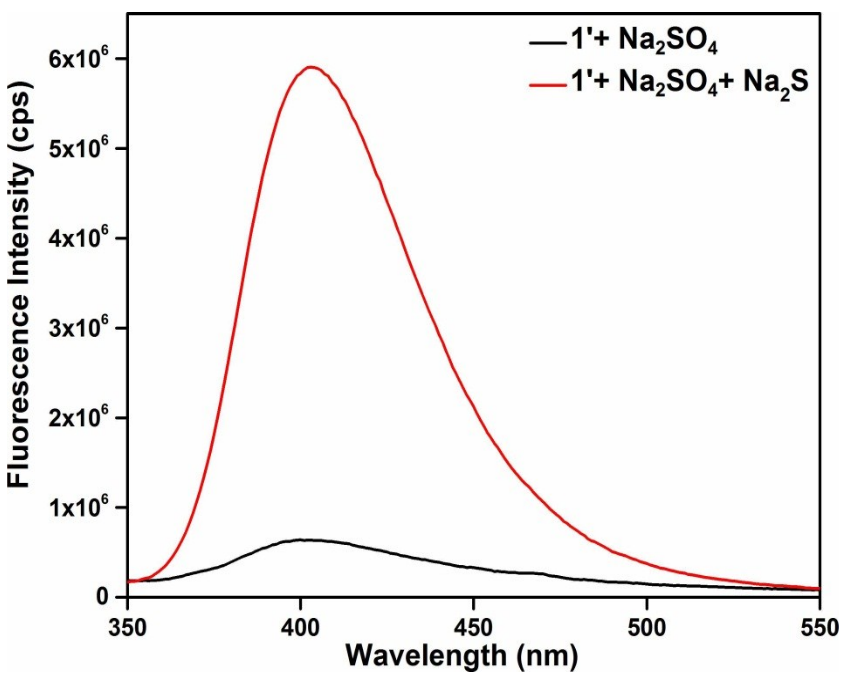

Figure S33. Fluorescence response of **1′** towards Na_2S in presence of Na_2SO_4 (λ_{ex} = 330 nm and λ_{em} = 405 nm).

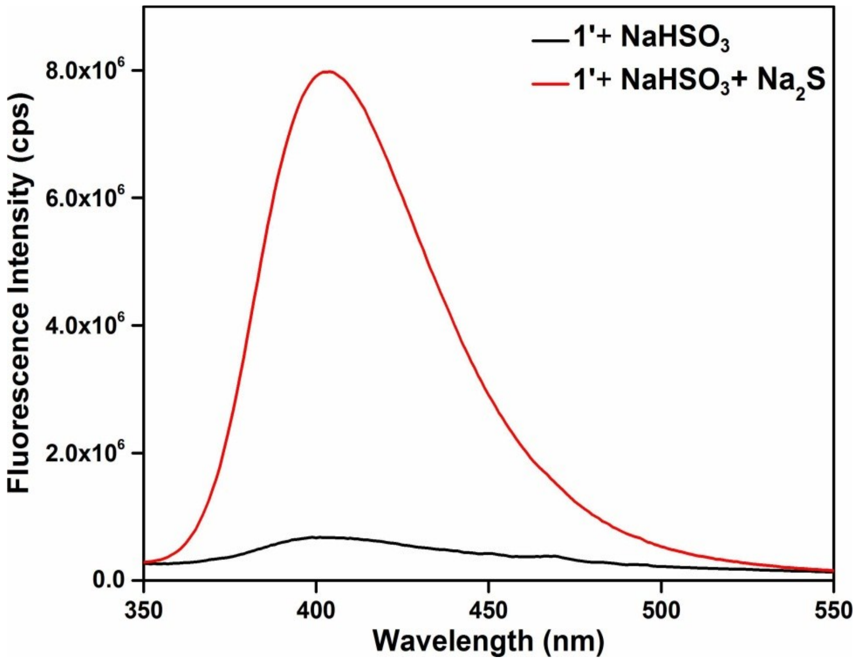

Figure S34. Fluorescence response of **1′** towards Na_2S in presence of $NaHSO_3$ (λ_{ex} = 330 nm and λ_{em} = 405 nm).

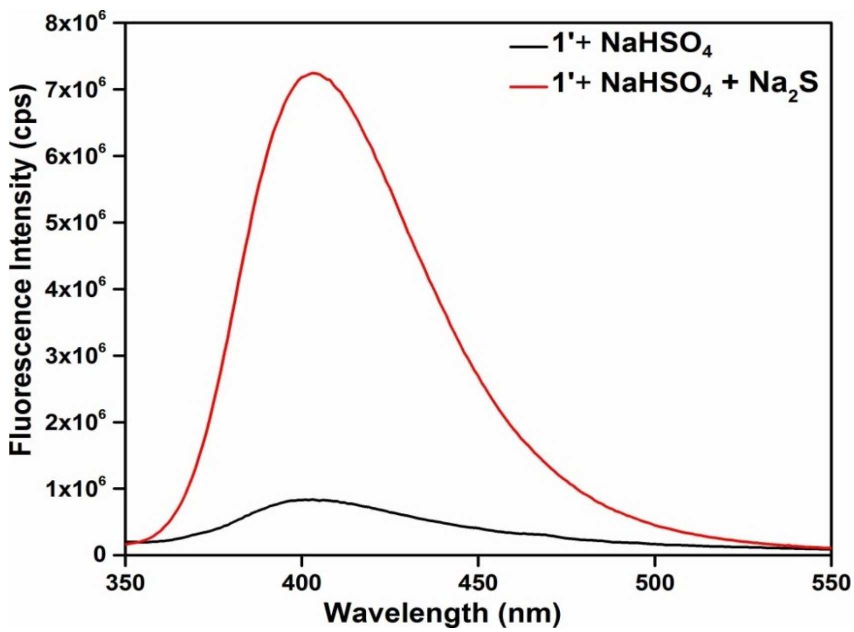

Figure S35. Fluorescence response of **1′** towards Na_2S in presence of $NaHSO_4$ (λ_{ex} = 330 nm and λ_{em} = 405 nm).

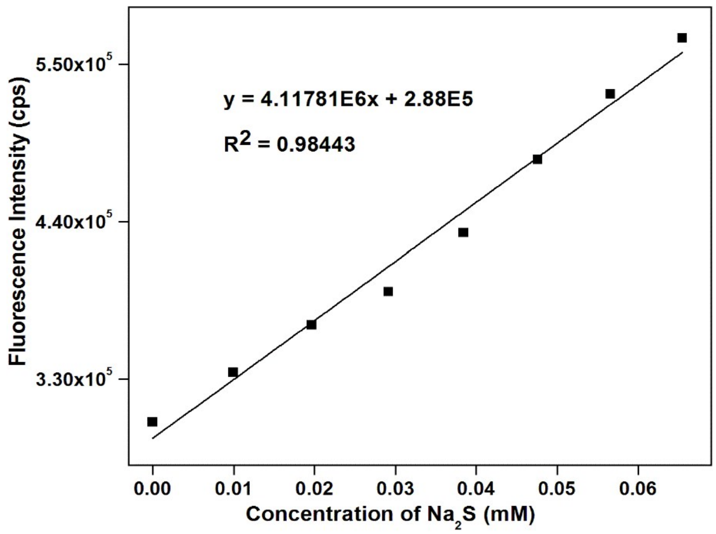

Figure S36. Change in the fluorescence intensity of **1′** in 10 mM HEPES buffer as a function of concentration of Na_2S.

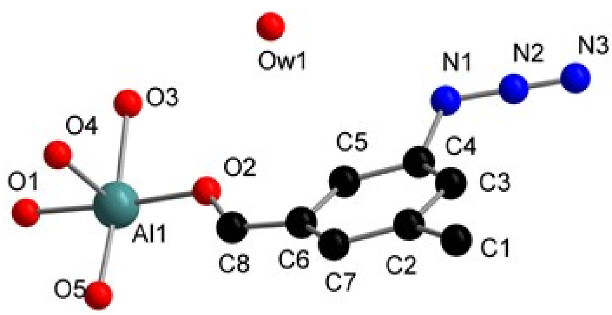

Figure S37. The asymmetric unit of **1** with numbering scheme as used below. Please note that standard uncertainties for fragments refined as rigid bodies are not given.

Al1	O5	1.822(25)
	O5	1.831(26)
	O1	1.917(21)
	O2	1.932(21)
	O4	1.936(20)
	O3	1.975(21)
O1	C1	1.222(26)
O2	C8	1.253(27)
O3	C8	1.260(29)
O4	C1	1.240(26)
C1	C2	1.405(19)
C2	C3	1.4024
	C7	1.4044
C3	C4	1.3955
C4	C5	1.3887
	N1	1.4561

	C2	1.4024
C5	C6	1.4009
C6	C7	1.4037
	C8	1.427(20)
N1	N2	1.2311
N2	N3	1.1192
Ow1	N3	3.278(30)

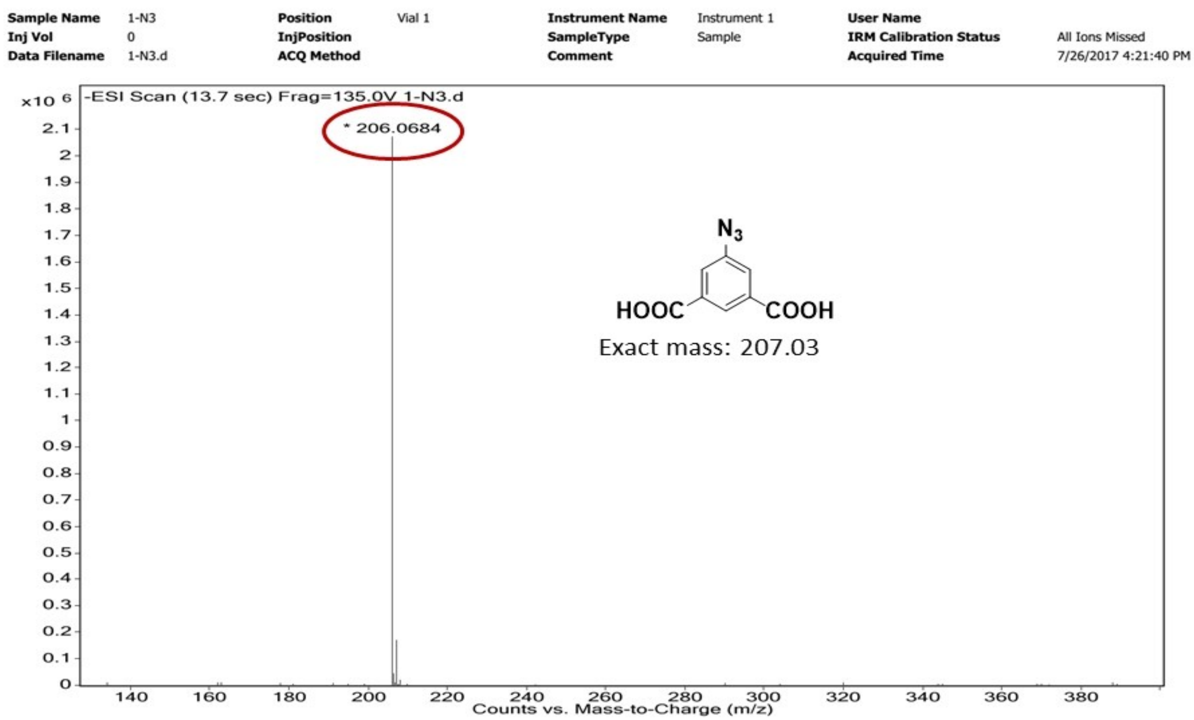

Figure S38. HR-MS spectrum of un-treated **1′** after digestion in MeOH/HF. The spectrum shows m/z (negative ion mode) peak at 206.0684, which corresponds to $(M-H)^-$ ion (M = mass of H_2IPA-N_3 ligand).

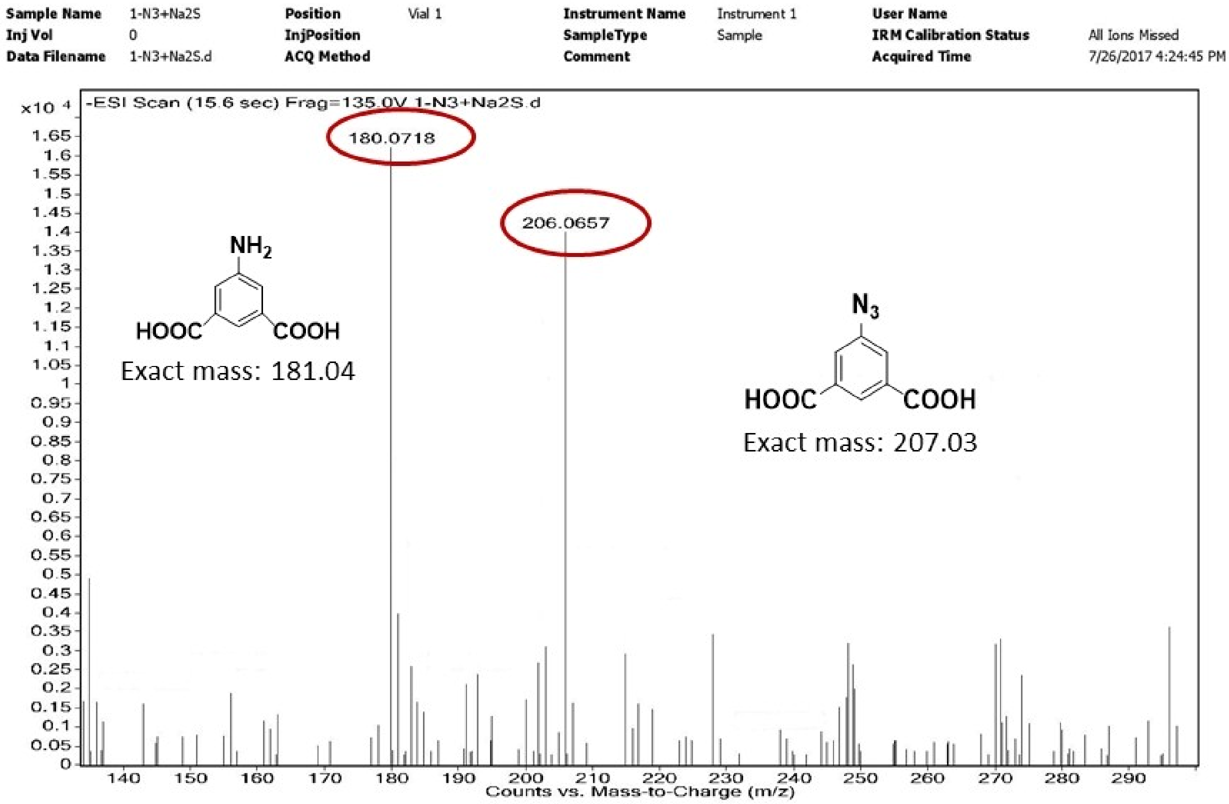

Figure S39. HR-MS spectrum of Na_2S-treated **1′** after digestion in MeOH/HF. The spectrum shows m/z (negative ion mode) peaks at 206.0657 and 180.0718, which correspond to $(M\text{-}H)^-$ ion of $H_2IPA\text{-}N_3$ and reduced $H_2IPA\text{-}N_3$ (i.e. $H_2IPA\text{-}NH_2$) ligands, respectively.

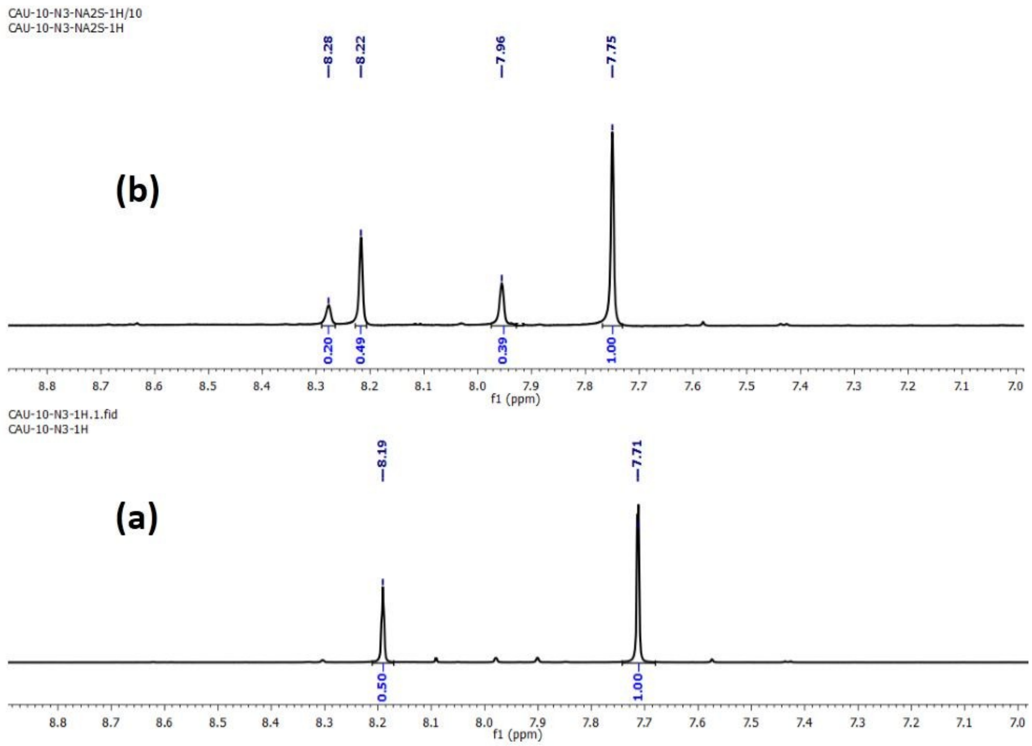

Figure S40. ^{1}H NMR spectra of (a) un-treated **1′** and (b) Na_2S-treated **1′** after digestion in DMSO-d_6/HF. Compared to un-treated **1′**, new peaks for H_2IPA-NH_2 ligand arise at 7.96 and 8.28 ppm in case of Na_2S-treated **1′**, which prove partial conversion of azide functionality into amine. To calculate the percent of conversion, the peak corresponding to two equivalent aromatic protons of H_2IPA-N_3 ligand is set to an integration of 1 and all new peaks are integrated accordingly. For Na_2S-treated **1′**, the integrations of the new peaks are approx. ~0.39 and ~0.20 with respect to two equivalent aromatic protons of H_2IPA-N_3 ligand. Hence, percentage conversion of azide to amine is ~28%.

Table S1. Structural refinement parameters for **1**.

formula	$AlO_5C_8H_3N_3$
crystal system	tetragonal
space group	$I4_1/a$
a / Å	21.4250(14)
c / Å	10.7954(11)
V/ Å^3	4955.4(7)
R_{wp} / %	4.7
R_p / %	3.5
R_{Bragg} / %	1.8
GoF	2.8

Table S2. Comparison of the response time, detection limit and analyte used for the detection of H_2S by MOFs reported till date.

Sl. No.	MOF	Response Time (s)	Detection Limit (μM)	Analyte	Ref.
1	CAU-10-N_3	420	2.65	Na_2S	This work
2	DUT-52-$(NO_2)_2$	3300	20.0	Na_2S	1
3	Ce-UiO-66-N_3	760	12.2	NaSH	2
4	Ce-UiO-66-NO_2	760	34.84	NaSH	2
6	IRMOF-3-N_3	< 120	28.3	NaSH	3
7	Zr-UiO-66-NO_2	≈ 460	188	Na_2S	4
8	Zr-UiO-66-N_3	180	118	Na_2S	5
9	MN-ZIF-90	-	-	-	6
10	Al-TCPP-Cu	-	-	-	7
11	Al-MIL-101-N_3	-	100 (UV-lamp excitation); 0.1 (laser excitation)	Na_2S	8
12	Eu^{3+}/Cu^{2+}@UiO-66-$(COOH)_2$	30	5.45	NaSH	9

Table S3. Comparison of the concentration of biological analytes found in real system and in sensing medium of this work.

Sl. No.	Analytes	Concentration of Analyte in Human Blood (mg/mL)	Concentration of Analyte Added to the Sensing Medium of This Work (mg/100 μL)[#]	Final Concentration of Analyte in Sensing Medium of This Work (mg/mL)	Ref.
1	chloride (Cl^-)	5.87	1.04	0.48	10
2	bromide (Br^-)	(2.5-11.7) $\times 10^{-3}$	1.83	0.86	11
3	iodide (I^-)	(14.1-812) $\times 10^{-6}$	2.6	1.22	12
4	alanine	3.41×10^{-2}	1.58	0.74	13
5	serine	1.12×10^{-2}	1.87	0.87	13
6	cysteine	1.18×10^{-2}	2.15	1.01	13
7	glutathione	0.33-0.24	5.47	2.57	14

[#] Concentration of each analyte added to the sensing medium = 17.8 μmol/100 μL (10 equivalents with respect to the azide functionality).

Crystallographic Information File (CIF) for Compound 1:

```
data_compound1
_chemical_name_CAU-10-N3
_cell_length_a  21.4250(14)
_cell_length_b  21.4250(14)
_cell_length_c  10.7954(11)
_cell_angle_alpha 90
_cell_angle_beta  90
_cell_angle_gamma 90
_cell_volume 4955.42(81)
_symmetry_space_group_name_H-M I41/A
loop_
_symmetry_equiv_pos_as_xyz
        '-x, -y+1/2, -z+1/4'
        '-x+1/2, -y+1/2, z+1/2'
        '-y, x+1/2, z+1/4'
        '-y+1/2, x+1/2, -z+1/2'
        'y, -x, -z'
        'y+1/2, -x, z-1/4'
        'x, y, z'
        'x+1/2, y, -z-1/4'
        '-x+1/2, -y, -z-1/4'
        '-x, -y, z'
        '-y+1/2, x, z-1/4'
        '-y, x, -z'
        'y+1/2, -x+1/2, -z+1/2'
        'y, -x+1/2, z+1/4'
        'x+1/2, y+1/2, z+1/2'
        'x, y+1/2, -z+1/4'
loop_
_atom_site_label
_atom_site_type_symbol
_atom_site_symmetry_multiplicity
_atom_site_fract_x
_atom_site_fract_y
_atom_site_fract_z
_atom_site_occupancy
_atom_site_B_iso_or_equiv
Al1 Al   0 0.24869(76) 0.31596(52) 0.3680(13) 1 0.56(30)
O1 O   0 0.16007(62) 0.31666(72) 0.3922(15) 1 0.56(30)
O2 O   0 0.33766(62) 0.32074(77) 0.3405(16) 1 0.56(30)
O3 O   0 0.23356(80) 0.38401(83) 0.2483(13) 1 0.56(30)
O4 O   0 0.25485(71) 0.38073(71) 0.4924(13) 1 0.56(30)
O5 O   0 0.26052(84) 0.25821(81) 0.4896(23) 1 0.56(30)
C2 C   0 0.5611108 0.2891358 0.3697755 1 3.63(46)
C5 C   0 0.4477892 0.3096717 0.2490943 1 3.63(46)
C1 C   0 0.62364(87) 0.2795(11) 0.4041(21) 1 3.63(46)
C3 C   0 0.5595848 0.3034112 0.2430319 1 3.63(46)
C7 C   0 0.5049743 0.2851878 0.4364835 1 3.63(46)
C8 C   0 0.38245(93) 0.2976(11) 0.3994(24) 1 3.63(46)
C6 C   0 0.4479794 0.29574 0.3758802 1 3.63(46)
C4 C   0 0.5029958 0.3132339 0.1820676 1 3.63(46)
```

N1 N 0 0.4954411 0.3467218 0.06565453 1 3.63(46)
N2 N 0 0.5424529 0.3442848 0.0002683282 1 3.63(46)
N3 N 0 0.5851322 0.3419312 -0.05932386 1 3.63(46)
Ow1 O 0 0.4300(14) 0.4524(13) 0.2962(27) 1.000(31) 3.63(46)

References:

1. R. Dalapati, S. N. Balaji, V. Trivedi, L. Khamari and S. Biswas, *Sens. Actuators., B*, 2017, **245**, 1039-1049.
2. A. Buragohain and S. Biswas, *CrystEngComm*, 2016, **18**, 4374-4381.
3. X. Zhang, J. Zhang, Q. Hu, Y. Cui, Y. Yang and G. Qian, *Appl. Surf. Sci.*, 2015, **355**, 814.
4. S. S. Nagarkar, A. V. Desai and S. K. Ghosh, *Chem. Eur. J.*, 2015, **21**, 9994-9997.
5. S. S. Nagarkar, T. Saha, A. V. Desai, P. Talukdar and S. K. Ghosh, *Sci. Rep.*, 2014, **4**, 7053-7058.
6. H. Li, X. Feng, Y. Guo, D. Chen, R. Li, X. Ren, X. Jiang, Y. Dong and B. Wang, *Sci. Rep.*, 2014, **4**, 4366-4370.
7. Y. Ma, H. Su, X. Kuang, X. Li, T. Zhang and B. Tang, *Anal. Chem.*, 2014, **86**, 11459-11463.
8. A. Legrand, A. Pastushenko, V. Lysenko, A. Geloen, E. A. Quadrelli, J. Canivet and D. Farrusseng, *ChemNanoMat*, 2016, **2**, 866-872.
9. X. Zhang, Q. Hu, T. Xia, J. Zhang, Y. Yang, Y. Cui, B. Chen and G. Qian, *ACS Appl. Mater. Interfaces*, 2016, **8**, 32259–32265.
10. H. C. Gram, *J. Biol. Chem.*, 1924, **61**, 337-343.
11. H. A. Olszowy, J. Rossiter, J. Hegarty and P. Geoghegan, *J. Anal. Toxicol.*, 1998, **22**, 225-230.
12. T. Zhang, Q. Wu, H. W. Sun, J. Rao and K. Kannan, *Environ. Sci. Technol.*, 2010, **44**, 6947-6953.
13. W. H. Stein and S. Moore, *J. Biol. Chem.*, 1954, **211**, 915-926.
14. F. Michelet, R. Gueguen, P. Leroy, M. Wellman, A. Nicolas and G. Siest, *Clin. Chem.*, 1995, **41**, 1509-1517.